Degradation of Cyanide using Stabilized S, N-TiO2 Nanoparticles by Visible and Sun Light

Article *in* Journal of Advanced Oxidation Technologies · January 2018

DOI: 10.26802/jaots.2017.0101

3 authors, including:

Mehraban Sadeghi
Shahrekord University of Medical Sciences
16 PUBLICATIONS **19** CITATIONS
SEE PROFILE

Neda Masoudipour
Shahrekord University of Medical Sciences
6 PUBLICATIONS **48** CITATIONS
SEE PROFILE

Open Access

Journal of Advanced Oxidation Technologies 2018; 21(1)
Article ID- 20170101

Article:

Degradation of Cyanide using Stabilized S, N-TiO_2 Nanoparticles by Visible and Sun Light

Fazel Mohammadi-Moghadam[1], Mehraban Sadeghi[2], Neda Masoudipour[*, 3]

[1-3] Department of Environmental Health of Engineering, School of Health, Shahrekord University of Medical Sciences, P.O. Box 88155-383, Shahrekord, Iran

[1]fazel.health@gmail.com; [2]sadeghi@skums.ac.ir; [*,3]n.masoudipour@yahoo.com

Abstract

In this paper, cyanide degradation (at pH12) using S, N-TiO_2 photo-catalyst, synthesized by sol-gel method, stabilized on glass microbeads and scoria stones were investigated. The main raw materials were thiourea (Tu) as a source of S and N and tetra butyl orthotitanate (TBOT). The effects of S and N amount, visible and sun light, irradiation time and different initial cyanide concentrations (50, 100, 200 and 300 mg/L) on destruction of cyanide were studied. The S, N-TiO_2 film with 0.25 g thiourea showed the best cyanide destruction in visible light. The results showed that cyanide (50 mg/L) was destructed up to 94% in visible light and approximately 100% in sun light by S, N-TiO_2/glass microbead. The results also indicated 85% and 94% destruction in visible and sun light respectively by S, N-TiO_2/scoria stone within 4 h. Finally, the S, N-TiO_2 stabilized on glass microbeads can be effectively implemented as a new method for treatment of wastewater containing free cyanide under sun light.

Keywords

Photo-catalysis; Heterogeneous Photo-catalysis; Cyanide; Sunlight

Received: September 24, 2017; **Revised:** November 01, 2017; **Accepted:** November 16, 2017

Introduction

Global water shortage and population growth, on the one hand, and surface and groundwater contamination resulting from toxic wastewaters discharge, on the other hand, gives the priority to wastewater treatment methods and the possibility of reusing it in environmental studies.

Cyanide (CN^-) is one of the most toxic pollutants in industrial wastewaters. This compound exists in wastewater of electroplating, metal finishing, automobile parts manufacture, plating, pharmaceuticals, coal gasification, plastics, production of chemicals such as pesticides, nitrile, nylon and acrylic and extraction of gold and silver [1-4]. According to US-health service, permissible limit and guideline of CN^- in effluent are 0.2 mg/L and 0.01mg/L respectively [5, 6]. In view of the negative effects of cyanide on health, processes have been developed for the removal of cyanide, such as use of azotobacter and other microorganisms in activated sludge system, dilution, electrochemical processes, hydrolysis and distillation, adsorption by activated carbon, resins and membranes, acidification/evaporation, increasing metals, flotation and solvent extraction, alkaline chlorination, sulfur dioxide, etc. [7-12]. Implementation of some processes may face barriers like the high cost of treatment, need for additional treatment, low efficiency, sludge disposal, usability for limited range of concentrations, and generation of toxic byproducts [13]. Advanced oxidation processes (AOPs) such as oxidation with hydrogen peroxide (H_2O_2), ozone (O_3), ultrasound, fenton, and photo-catalysts such as TiO_2 and ZnO have been put forward in recent years as the new methods of treating wastewater containing CN^-. TiO_2 can be used over and over without any decrease in its

DOI: 10.26802/jaots.2017.0101

photo-catalytic activity as a non-toxic catalyst. Nano-size TiO_2, due to its high surface to volume ratio, increases the density of active sites and reduces recombination bulk [2, 14-17]. Exposure to the light containing energy equal to or more than TiO_2 corresponding band gap leads to the electron excitation from the valence band to the conduction band. This mechanism generates electron/hole pairs [18]. According to the studies conducted so far, there are two mechanisms for photo-catalytic oxidation of CN^- by TiO_2; heterogeneous charge transfer by the reaction of adsorbed CN^- with holes and the homogeneous pathway by adsorbed OH^- or defused OH^- [19]. According to the equations 1 to 4, the result of CN^- photo-catalytic oxidation is the formation of less toxic cyanate (CNO^-) which is finally converted into Carbon dioxide (CO_2) and Nitrate (NO_3^-) [20-22].

$$CN^- \rightarrow CN^{\cdot} \quad (1)$$

$$2CN^{\cdot} \rightarrow (CN)_2 \quad (2)$$

$$(CN)_2 + 2OH^- \rightarrow CN^- + CNO^- + H_2O \quad (3)$$

$$CNO^- + 8OH^- + 8h^+ \rightarrow NO_3^- + CO_2 + 4H_2O \quad (4)$$

In spite of all the effective photo-catalytic results with TiO_2 powder during the past 30 years, some practical problems associated with the usage of powder, such as stirring constantly working solution, post separation costs for TiO_2 particles recovering, filtration of solution after each run and shadowing effect, focused the efforts to work on stabilization of TiO_2 particles on substrates like glass beads, glass fiber, silica, zeolites, activated carbon and nanotubes [23-27]. Solar light (40% visible, 3% ultraviolet and 57% infrared) is an economically efficient source of energy. However, due to the poor activity of TiO_2 polymorphs (anatase and rutile) in visible light resulting from their wide band gap, their usage is limited in solar light utilization [28]. Non-metal doping of TiO_2 (N, C, S, and F) has been quite effective in improving the TiO_2 photo-catalytic activity in solar light [29-31].

In this study, we used an innovative method for CN^- destruction by stabilized S, N-TiO_2 on two substrates. At first, the sol-gel dip-coating technique was used for S, N-TiO_2 stabilization on glass microbeads and scoria stones. Then, the photo-catalytic destruction of CN^- was investigated under visible and sun light irradiation in four different CN^- concentrations ranging from (50 to 300 mg/L).

Materials and Methods

Preparation of Photo-catalysts

All the chemicals were provided by Merck Company and used without any further purification. Deionized (DI) water was prepared by single water stills, GFL, Germany.

According to the method used by Behpour et al, TiO_2 and S, N-TiO_2 nanoparticles were synthesized by sol-gel method [32]. The TiO_2 sol was prepared by hydrolyzing tetrabutylorthotitanate (TBOT) in acidic solution. In this method, 2.5 mL TBOT, 10 mL ethanol and 2.5 mL acetylacetone (Acac) were mixed. Acac was used for controlling hydrolysis reaction rate. After 30 min of stirring, the clear and yellow solution was obtained. Then, 2.0 mL DI water was added to it and the solution was stirred for 10 min. In order to adjust the pH of sol at about 1.8, the concentrated HCl was added. Thiourea (Tu) was used as a source of nitrogen and sulfur, and three different quantities of Tu including 0.10, 0.25 and 0.40 g were added to prepared sol. The presence of Tu in the synthetic sol causes the TiO_2 photo-catalytic activity to transfer to visible light. After stirring for 2 h, the stable sol was achieved. This solution was prepared to stabilize on substrates. The used substrates were glass microbeads (diameters 450-550 μm) and scoria stones. The glass microbeads were washed by detergent and immersed in diluted HCl solution for 8 h and were subsequently rinsed out with DI water and dried in the oven at 105 ^{0}C for 2 h. In order to remove the Fe in scoria stones, the stones were digested in concentrated HCl for 72 hours afterward, were carefully washed out with DI water and finally, were placed in theoven for 24 h to dry at 105 ^{0}C. The as-dip-coated films were put in the oven at 60 ^{0}C for four hours. These samples were calcinated at 500 ^{0}C for 1 h.

Characterization

The band gap of the samples was estimated by diffuse reflectance UV–Vis spectroscopy (UV/Vis-DRS) using a

Shimadzu UV-1800 spectrophotometer and applying equation 5:

$$E_g = \frac{1239.8}{\lambda} \quad (5)$$

Where E_g is the band gap (eV) and λ is the wavelength (nm) of the absorption edges in the spectrum [2].

X-ray diffraction (XRD) analysis was applied for determining the crystalline size and structure of the prepared thin films with Philips X'pert Pro MPD using Cu kα radiation as the X-ray source in the 2θ range of 10–80°. The average crystallite size of anatase phase was estimated by equation 6 (Schererr equation).

$$S = \frac{K\lambda}{\beta cos\theta} \quad (6)$$

Where S is the mean crystalline dimension, K the crystalline shape constant (0.89), θ the diffraction angle at the maximum peak, λ The X-ray wavelength (Cu kα), and β is the full width at half maximum of the peak in radians [12].

The surface morphology of the TiO_2 films was observed on scanning electron microscopy (SEM) (Zeiss EVO"15) equipped with an energy dispersive X-ray (EDX) for elemental analysis.

Photo-catalysis Experiments

Destruction of CN^- by synthesized photo-catalysts was investigated under visible and sun light. The experiments were carried out using 5 glass tubes (height 200 mm and diameter 8 mm) filled with 50 g TiO_2 and S, N-TiO_2 on glass microbeads and scoria stones in separate sets of tests. The glass tubes were fixed over a mirror standing on a board. Fig. 1 shows the reactor used in photo-catalytic experiments in sun light.

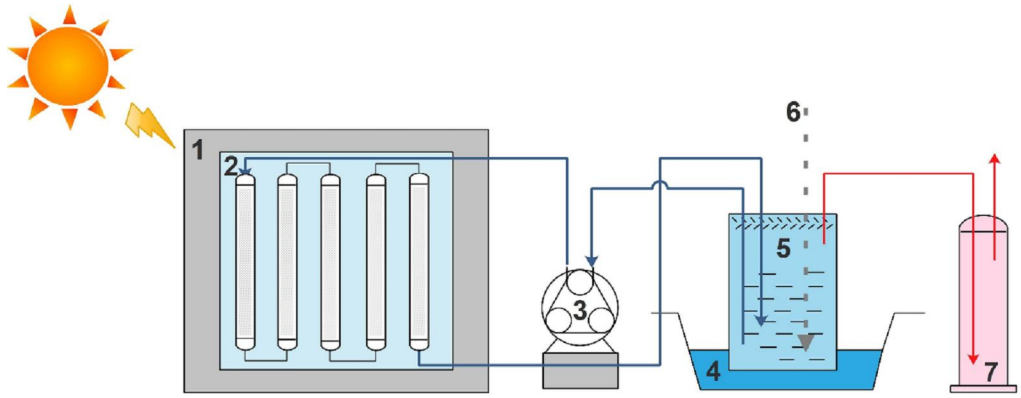

FIG. 1 SCHEMATIC REPRESENTATION OF THE PHOTO-REACTOR: (1) SOLAR BOARD, (2) GLASS TUBES AND MIRROR, (3) PERISTALTIC PUMP, (4) THERMOSTATIC WATER BATH, (5) CN^- VESSEL, (6) AIR, (7) HCN SCRUBBER

1000 mL of CN^- solution was pumped with a flow rate of 200 mL/min. the photo-catalysts were reused for several times with new stock solutions. The filled glass tubes were irradiated by visible light (lamp) with intensity 400 W/m^2 and sun light (under the clear sky in June). The distance between the glass tubes and the lamp was 20 cm. The experiments were carried out isothermally at 30 °C. The air was bubbled into the CN^- solution throughout the experiments to make sure there are sufficient electron scavengers present to trap the excited conduction band electron in order to prevent the e^-/h^+ recombination, stabilization of radical intermediates and stirring the CN^- solution [18, 33].

Photo-catalytic experiments were performed with different initial CN^- concentrations including 50, 100, 200 and 300 mg/L at 4 h contact time. The pH of all solutions was adjusted at 12 by diluted NaOH and HCl to prevent the HCN gas production [34]. The HCN gas produced during the experiments was trapped by the 1 M NaOH solution. The CN^- concentration was estimated by volumetric titration with $AgNO_3$, using p-dimthylaminobenzalrhodanine to determine the end point of titration [35]. The CN^- photo-catalytic destruction was calculated using equation 7,

$$CN^{-}photocatalytic\ destruction\ (\%) = \frac{(C_0 - C)}{C_0} \times 100 \quad (7)$$

Where C_0 is the initial concentration of CN^-, and C is the concentration of remaining CN^- in the solution.

The calculation of sample size in this study was conducted, using the full factor method. Each series of experiments was repeated twice in order to evaluate the repeatability of the method and cyanide measurement tests were done by titration three times. Considering the number of variables and repeated tests, 384 tests were performed altogether. In order to compare the action of variables on cyanide destruction, the research data was evaluated by independent T-test using SPSS software.

Results and Discussion

Morphological, Compositional and Structural Characterizations

The XRD patterns of pure TiO_2, S, N-TiO_2 film on glass microbead and S, N-TiO_2 film on scoria stone are shown in Fig. 2. It can be seen most of the sharp peaks in this figure are the diffractions of TiO_2 anatase phase according to the joint committee on powder diffraction standards No. 04-0477 [36]. No peak for Nitrogen and Sulfur was observed in Fig. 2 (b) and (c) because of low concentrations and good dispersion of their on anatase phase.

The average crystal sizes of TiO_2 and S, N-TiO_2 films on glass microbead and scoria stone that were calculated according to equation 2 using the 101 peak, obtained 8-10, 11-19 and 11-17 nm, respectively.

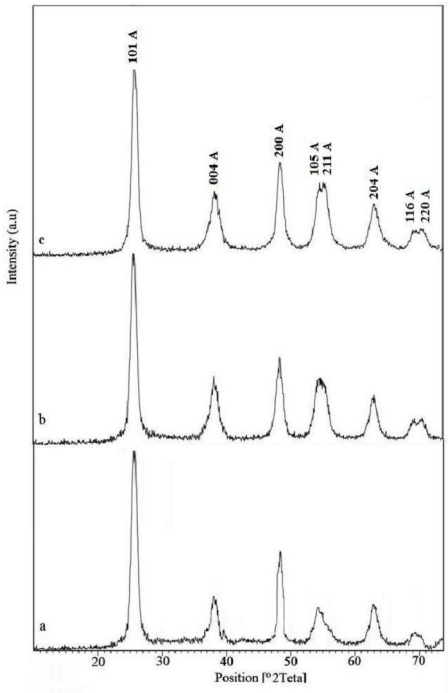

FIG. 2 XRD PATTERNS OF THE FILM OF (A) TIO_2, (B) S, N-TIO_2 ON GLASS MICROBEAD AND (C) S, N-TIO_2 ON SCORIA STONE

The SEM images of synthesized TiO_2 and S, N-TiO_2 films on glass microbead and scoria stone has been shown in Fig. 3. The nanometric particle size of TiO_2 and S, N-TiO_2 films is clearly seen in Fig. 3.

In general, the nano-size photo-catalyst particles tend to aggregate due to van der Waals attraction existing between the particle surfaces [23]. Moreover, according to the work of Wang et al, the increase of Tu results in agglomeration of nanometric particles in some areas [37], which can be seen in Fig. 3 (b) and (d).

Furthermore, the photo-catalysts film on glass microbead compared to the film on scoria stone was more uniform due to the smoother surface.

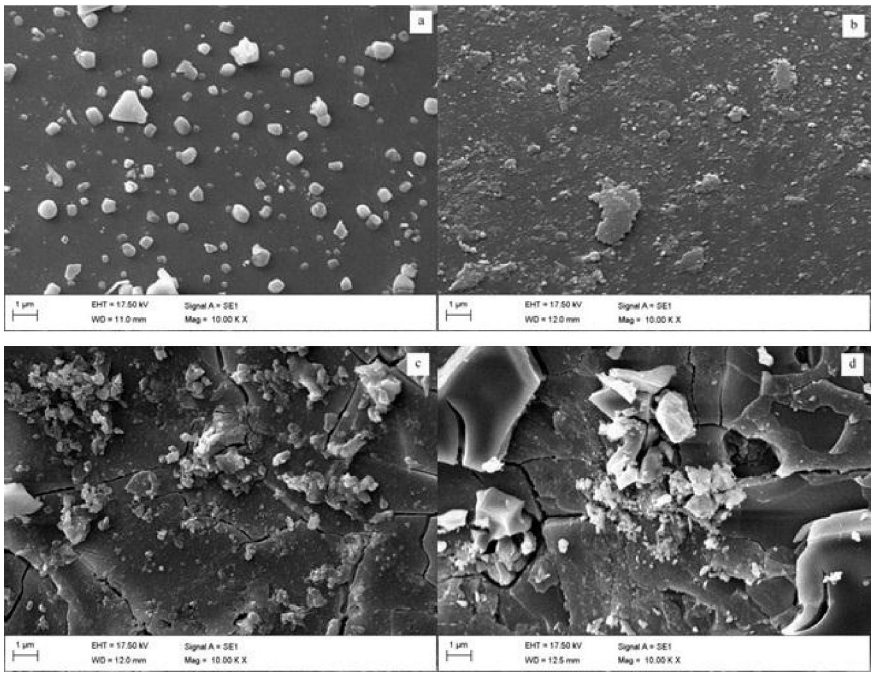

FIG. 3 SEM IMAGES OF FILMS OF (a) TiO_2 ON GLASS MICROBEAD, (b) S, N-TiO_2 ON GLASS MICROBEAD, (c) TiO_2 ON SCORIA STONE AND (d) S, N-TiO_2 ON SCORIA STONE

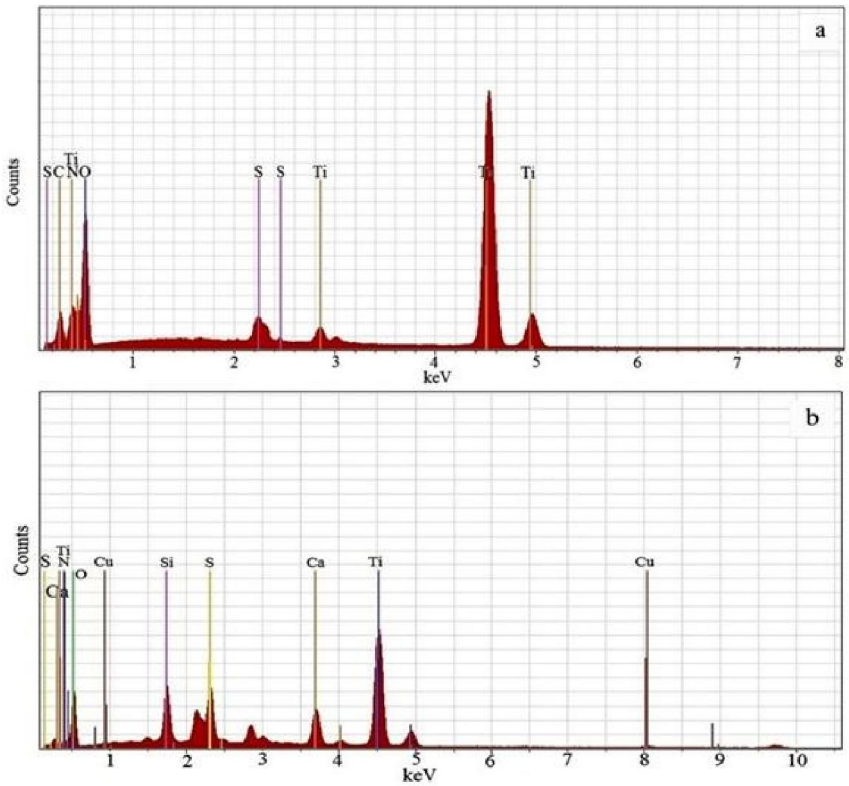

FIG. 4 EDX ANALYSIS OF FILM OF (a) S, N-TiO_2 ON GLASS MICROBEAD AND (b) S, N-TiO_2 ON SCORIA STONE

The EDX analysis of S, N-TiO_2 film on glass microbead and scoria stones is shown in Fig. 4 (a) and (b), respectively. This pattern has confirmed the presence of nitrogen and sulfur due to the existence of Tu in S, N-TiO_2 film.

In Fig. 4 (b), in addition to Ti, O, N and S peaks, the Cu, Si and Ca peaks were also visible due to some surficial cracks extended in scoria stone.

Optical Characterization

The DRS spectra of different quantities of Tu added to TiO_2 are presented in Fig. 5. The absorption threshold of the TiO_2 film (0.00 g Tu) was 380 nm, which according to equation 1 is corresponding to a band gap of 3.26 eV. The absorptions obtained from three different quantities of Tu (0.10, 0.25 and 0.40 g), added to TiO_2, and whose calculated band gap energies are equal to 3.18, 3.15 and 3.08 eV are 390, 394 and 402 nm, respectively.

According to studies done by Baeissa, Behpour et al, Qin et al, the band gap narrowing have been resulted from the mixture of nonmetal p and TiO_2 O 2p orbitals [2, 28, 37, 38]. In fact, Tu has been led to the red shift of TiO_2 absorption edge toward the visible region.

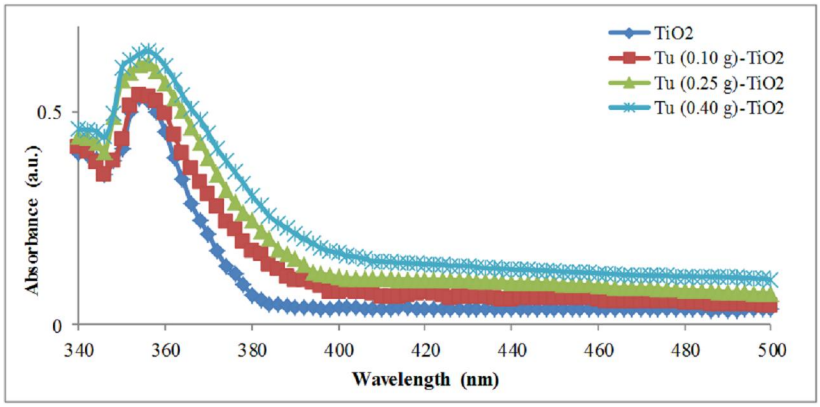

FIG. 5 DRS SPECTRA OF S, N-TiO_2 WITH DIFFERENT QUANTITIES OF Tu

CN- Removal by Synthesized Photo-catalysts

1) Effect of Tu Amount

Destruction using four different quantities of Tu including 0.00, 0.10, 0.25 and 0.40 g added to TiO_2 stabilized on glass microbead was investigated. The experiments were performed with 300 mg/L CN^- for 4 h, under visible light. The findings are displayed in Fig. 6. It is clearly seen that adding Tu to TiO_2, has enhanced the CN^- destruction. According to Fig. 6, adding 0.25 g of Tu to TiO_2 slightly has increased the CN^- destruction compared to 0.10 g; however, the CN^- destruction significantly has reduced when the Tu amount has increased to 0.40 g. According to other studies related to nonmetal doped TiO_2, the mentioned decrease results from the agglomeration of nanoparticles and the creation of obstacle in the path of light [2, 28, 34]. Hereinafter, the photo-catalyst used in experiments refers to Tu (0.25g)-TiO_2.

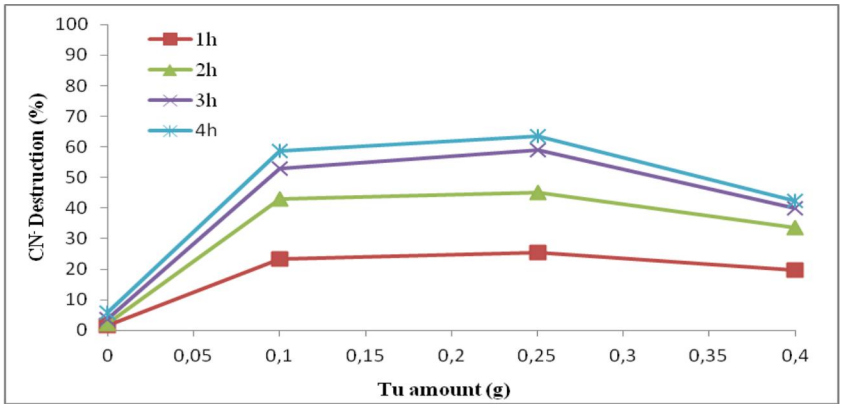

FIG. 6 CN^- PHOTO-DESTRUCTION PERCENT WITH DIFFERENT QUANTITIES OF Tu UNDER VISIBLE LIGHT

2) Effect of Initial CN^- Concentration

The effect of initial CN^- concentration on its destruction by S, N-TiO_2 stabilized on glass microbeads under

visible and sun light are shown in fig. 7 (a) and (b) respectively.

Fig. 8 (a) and (b) have illustrated the effect of initial CN^- concentration on its destruction under the same conditions using S, N-TiO_2 stabilized on scoria stone.

The reactions were carried out at four initial CN^- concentrations including 50, 100, 200 and 300 mg/L in both figures during 4 hours at pH12.

The maximum CN^- destruction rates obtained in fig. 7 (a) and (b) were 94.23% in visible and 99.65% in sun light and in fig. 8 (a) and (b) were 85.32% in visible and 94.20% in sun light after 4 h in lowest initial CN^- concentration.

According to Fig. 7 and Fig. 8, as initial CN^- concentration has increased, its destruction rate has significantly decreased and vice versa. Previous findings from related studies confirm this inverse relationship as well. The reason for this was that active sites of photo-catalyst are closed by CN^-, hence visible or sun light irradiations would not be able to penetrate into the photo-catalyst surface [39, 40].

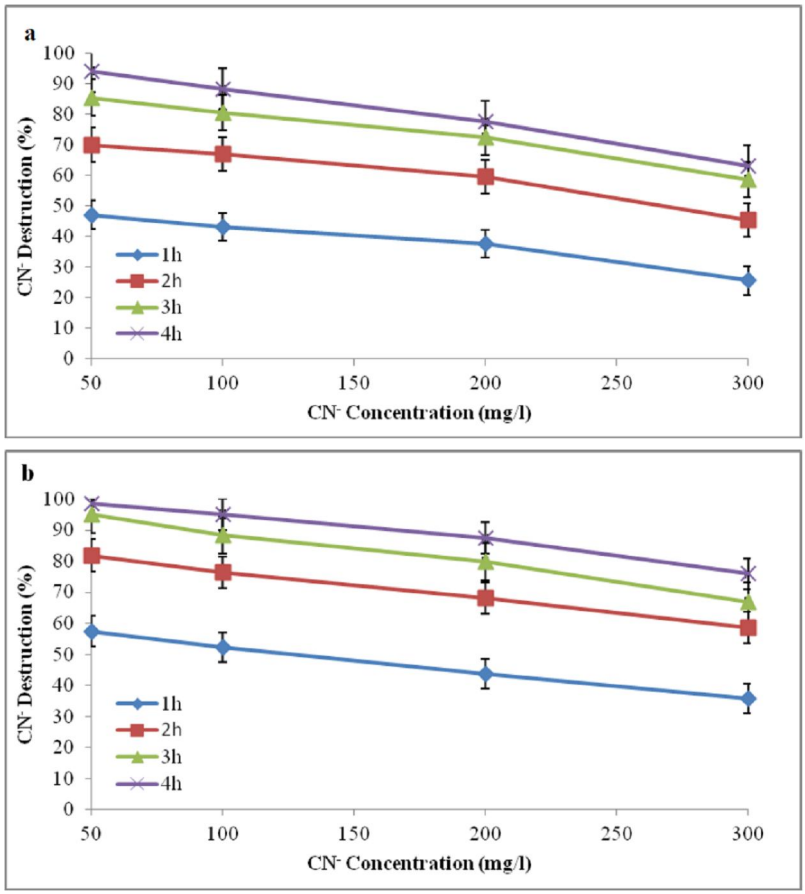

FIG. 7 CN^- PHOTO-DESTRUCTION PERCENT WITH DIFFERENT INITIAL CN^- CONCENTRATIONS IN PRESENCE OF S, N-TiO_2/GLASS MICROBEADS UNDER (a) VISIBLE LIGHT AND (b) SUN LIGHT

3) *Effect of Light Type*

Fig. 7 and Fig. 8 have demonstrated that the cyanide destruction rate using the photo-catalyst stabilized on glass microbeads in sun light, during four hours and in average, 4.42% is higher than the rate achieved in visible light. Also, the influence of sun light in the presence of photo-catalyst stabilized on scoria stone 8.88% was higher than it in visible light. The sun light was more influential compared to visible light maybe due to the presence of 3% ultraviolet spectrum, more comprehensiveness and intensity (1100-1120 W/m^2). Moreover, in the evaluation of independent T-test to compare the effect of sun and visible light on cyanide destruction by

stabilized photo-catalysts, the P-Values obtained for visible and sun light were 0.015 and 0.009 respectively. The results also show that there was a significant statistical difference in cyanide destruction under visible and sun light.

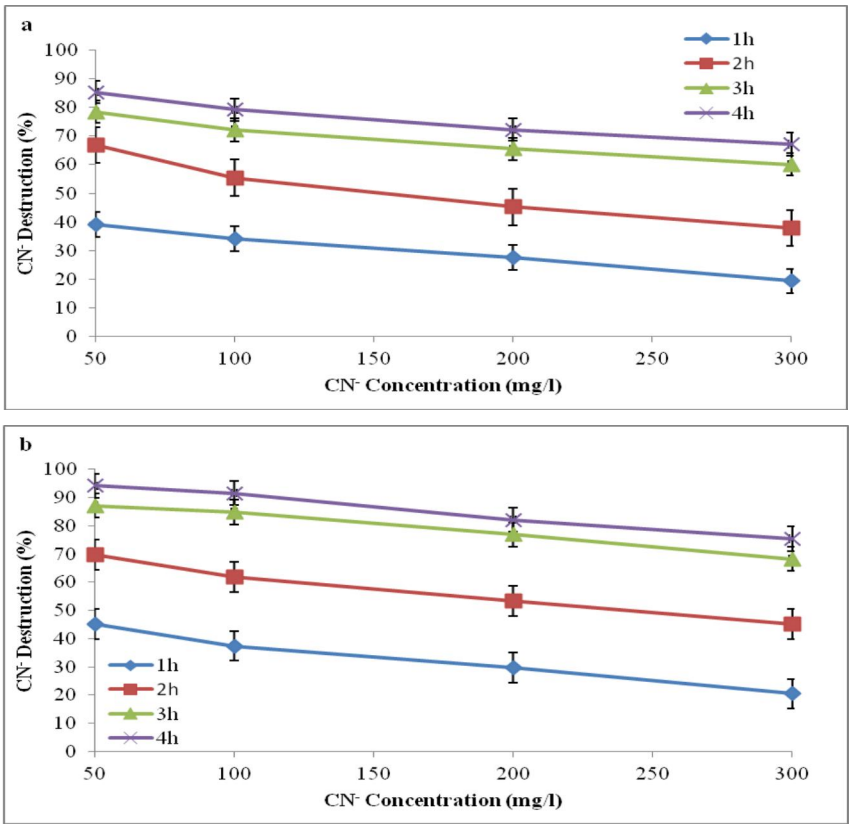

FIG. 8 CN^- PHOTO-DESTRUCTION PERCENT WITH DIFFERENT INITIAL CN^- CONCENTRATIONS IN PRESENCE OF S, N-TiO_2/SCORIA STONES UNDER (A) VISIBLE LIGHT AND (B) SUN LIGHT

4) *Effect of Substrate Type*

In Fig. 7 and Fig. 8, the comparison of substrate types (glass microbeads and scoria stones) indicated that the cyanide destruction rate by the photo-catalyst stabilized on glass microbeads and in average, during four hours in visible light about 8.91% and under sun light about 4.42% was higher than cyanide destruction rate by photo-catalyst stabilized on scoria stone. This might be related to higher transparency of glass microbeads than that of scoria stones. Probably, in scoria stone, despite its higher porosity and larger contact surface than glass microbead, due to its dark surface, the light could not pass through completely; hence the cyanide destruction rate is decreased. Also, considering the P-values 0.002 and 0.010 obtained for photo-catalysts stabilized on glass microbeads and scoria stone, it is clear that there was a significant statistical difference between cyanide destruction rates using these two substrates.

Conclusions

In this study, S, N-TiO_2 photocatalyst stabilized on glass microbead and scoria stones were synthesized by sol-gel method. Then, the CN^- photodestruction via synthetic catalyst stabilized on mentioned supporters was investigated separately.

The results were as follows:

- 0.25 g was the efficient quantity of thiourea as a source of N and S for the default value of TiO_2.

- The EDX proved the presence of S and N in photocatalysts.

- The DRS showed that thiourea leads to the red shift of TiO_2 absorption edge toward the visible region.

- The XRD results revealed that only the anatase TiO_2 formed in films and the particles size were in nanometric range.

- The SEM images confirmed the nanoparticle size of photocatalysts.

- The 50 ppm of cyanide concentration had the maximum photodestruction rate compared to higher concentrations.

- The type of light and substrate influenced the cyanide photodestruction rate; hence sun light and glass microbead had the best results.

Therefore, cyanide destruction via S, N-TiO_2 photo-catalyst stabilized on glass microbeads can be applied as an economically and environmentally acceptable method due to use of sunlight and nontoxic byproducts in industrial wastewater treatment.

ACKNOWLEDGEMENT

The authors would like to thank the vice-chancellor for research and technology at Shahrekord University of Medical Sciences for the financial support of this project.

REFERENCES

[1] E.S. Baeissa, Photocatalytic removal of cyanide by cobalt metal doped on TiO2-SiO2 nanoparticles by photo-assisted deposition and impregnation methods, Journal of Industrial and Engineering Chemistry, 20 (2014) 3761-3766.

[2] S.H.D.S. Baeissa, Synthesis and characterization of sulfur-titanium dioxide nanocomposites for photocatalytic oxidation of cyanide using visible light irradiation, Chinese Journal of Catalysis 36 (2015) 698-704.

[3] S.H. Do, Y.H. Jo, H.D. Park, S.H. Kong, Synthesis of iron composites on nano-pore substrates: Identification and its application to removal of cyanide, Chemosphere 89 (2012) 1450-1456.

[4] M. Farrokhi, J.K. Yang, S.M. Lee, M. Shirzad-Siboni, Effect of organic matter on cyanide removal by illuminated titanium dioxide or zinc oxide nanoparticles, Journal of Environmental Health Science and Engineering, 11 (2013) 23.

[5] R.M. Mohamed, I.A. Mkhalid, The effect of rare earth dopants on the structure, surface texture and photocatalytic properties of TiO2-SiO2 prepared by sol-gel method, Journal of Alloys and Compounds, 501 (2010) 143-147.

[6] C.A. Young, T.S. Jordan, Cyanide remediation: current and past technologies in: Proceeding of 10th annual on hazardous waste research, 2009.

[7] M. Botz, T. Mudder, A. Akcil, Cyanide treatment: physical, chemical and biological processes (Chapter 36), 2nd Edition - Advances in Gold Ore Processing ed., Elsevier Ltd., Amsterdam, 2015.

[8] X. Dai, P.L. Breuer, Cyanide and copper cyanide recovery by activated carbon, Minerals Engineering, 22 (2009) 469-476.

[9] R.R. Dash, A. Gaur, C. Balomajumder, Cyanide in industrial wastewaters and its removal: A review on biotreatment, Journal of Hazardous Materials, 163 (2009) 1-11.

[10] F. Gurbuz, F. Ciftci, A. Akcil, Biodegradation of cyanide containing effluents by Scenedemus obliquus, Journal of Hazardous Materials, 162 (2009) 74-79.

[11] B. Latkovaska, J. Figa, Cyanide removal from industrial wastewater, Polish Journal of Environmental Study, 16 (2007) 748-752.

[12] L. Szpyrkowicz, S.N. Kaul, E. Molga, M. DeFaveri, Comparison of the performance of a reactor equpped with a Ti/Pt and an SS anode for simultaneous cyanide removal and copper recovery, Electrochimica Acta, 46 (2000) 381-387.

[13] R.R. Dash, C. Balomajumder, A. Kumar, Removal of cyanide from water and wastewater using granular activated carbon, Chemical Engineering Journal, 146 (2009) 408-413.

[14] S. Murgolo, F. Petronella, R. Ciannarella, R. Comparelli, A. Agostiano, M.L. Curri, G. Mascolo, UV and solar-based photocatalytic degradation of organic pollutants by nano-sized TiO2 grown on carbon nanotubes, Catalysis Today 240

(2014) 114–124.

[15] L. Prieto-Rodriguez, S. Miralles-Cuevas, J. Oller, A. Aguera, G.L. Puma, S. Malato, Treatment of emerging contaminants in wastewater treatment plants (WWTP) effluents by solar photocatalysis using low TiO2 concentrations, Journal of Hazardous Materials, 211-212 (2012) 131-137.

[16] M.A. Sousa, C. Gonçalves, V.J.P. Vilar, R.A.R. Boaventura, M.F. Alpendurada, Suspended TiO2-assisted photocatalytic degradation of emerging contaminants in a municipal WWTP effluent using a solar pilot plant with CPCs, Chemical Engineering Journal, 198-199 (2012) 301-309.

[17] M.N. Sugihara, D. Moeller, T. Paul, T.J. Strathmann, TiO2-photocatalyzed transformation of the recalcitrant X-ray contrast agent diatrizoate, Applied Catalysis B: Environmental, 129 (2013) 114-122.

[18] M.A. Rauf, M.A. Meetani, S. Hisaindee, An overview on the photocatalytic degradation of azo dyes in the presence of TiO2 doped with selective transition metals, Desalination, 276 (2011) 13-27.

[19] K. Chiang, R. Amal, T. Tran, Photocatalytic oxidation of cyanide: kinetic and mechanistic studies, Journal of Molecular Catalysis A: Chemical, 193 (2003) 285-297.

[20] V. Augugliaro, V. Loddo, G. Marcì, L. Palmisano, M.J. López-Muñoz, Photocatalytic oxidation of cyanides in aqueous titanium dioxide suspensions, Journal of Catalysis, 166 (1997) 272-283.

[21] S.N. Frank, A.J. Bard, Heterogeneous photocatalytic oxidation of cyanide and sulfite in aqueous solutions at semiconductor powders, Journal of Physical Chemistry, 81 (1977) 1484-1488

[22] J.A. Pedraza-Avella, P. Acevedo-Peña, J.E. Pedraza-Rosas, Photocatalytic oxidation of cyanide on TiO2: An electrochemical approach, Catalysis Today, 135 (2008) 611-618.

[23] G. Laera, B. Jin, H. Zhu, A. Lopez, Photocatalytic activity of TiO2 nanofibers in simulated and real municipal effluents, Catalysis Today, 161 (2011) 147-152.

[24] G. Mascolo, R. Comparelli, M.L. Curri, G. Lovecchio, A. Lopez, A. Agostiano, Photocatalytic degradation of methyl red by TiO2: Comparison of the efficiency of immobilized nanoparticles versus conventional suspended catalyst, Journal of Hazardous Materials, 142 (2007) 130-137.

[25] N. Miranda-Garcia, S. Suarez, B. Sanchez, J.M. Coronado, S. Malato, M.J. Maldonado, Photocatalytic degradation of emerging contaminants in municipal wastewater treatment plant effluents using immobilized TiO2 in a solar pilot plant, Applied Catalysis B: Environmental, 103 (2011) 294-301.

[26] W. Zhang, L. Zou, L. Wang, A novel charge-driven self-assembly method to prepare visible-light sensitive TiO2/activated carbon composites for dissolved organic compound removal, Chemical Engineering Journal, 168 (2011) 485-492.

[27] H. Li, W. Zhang, L. Zou, L. Pan, Z. Sun, Synthesis of TiO 2–graphene composites via visible-light photocatalytic reduction of graphene oxide, Journal of Materials Research, 26 (2011) 970-973.

[28] M. Behpour, V. Atouf, Study of the photocatalytic activity of nanocrystalline S, N-codoped TiO2 thin films and powders under visible and sun light irradiation, Applied Surface Science, 258 (2012) 6595-6601.

[29] H. Li, J. Wang, S. Yin, T. Sato, Photocatalytic activity of (sulfur, nitrogen)-codoped mesoporous TiO2 thin films, Research in Chemical Intermediates, 36 (2010) 27-37.

[30] J.A. Rengifo-Herrera, C. Pulgarin, Photocatalytic activity of N, S co-doped and N-doped commercial anatase TiO2 powders towards phenol oxidation and E. coli inactivation under simulated solar light irradiation, Solar Energy, 84 (2010) 37-43.

[31] W. Zhang, L. Zou, L. Wang, Visible-light assisted methylene blue (MB) removal by novel TiO_2/adsorbent nanocomposites, Water Science and Technology, 61 (2010) 2863-2871.

[32] H. Khalilian, M. Behpour, V. Atouf, S.N. Hosseini, Immobilization of S, N-codoped TiO2 nanoparticles on glass beads for photocatalytic degradation of methyl orange by fixed bed photoreactor under visible and sunlight irradiation, Solar Energy, 112 (2015) 239-245.

[33] A. Fujishima, A. Honda, Electrochemical Photolysis of Water at a Semiconductor Electrode, Nature, 238 (1972) 37-38.

[34] K. Chiang, R. Amal, T. Tran, Photocatalytic degradation of cyanide using titanium dioxide modified with copper oxide, Advances in Environmental Research, 6 (2002) 471-485.

[35] APHA, WEF, APHA Method 4500-CN: Standard Methods for the Examination of Water and Wastewater, APHA, AWWA, WEF, 2012.

[36] D. Wang, B. Yu, F. Zhou, C. Wang, W. Liu, Synthesis and characterization of anatase TiO2 nanotubes and their use in dye-sensitized solar cells, Materials Chemistry and Physics, 113 (2009) 602-606.

[37] J. Wang, H. Li, H. Li, C. Zou, Mesoporous TiO2-xAy (A = N, S) as a visible-light-response photocatalyst, Solid State Sciences, 12 (2010) 490-497.

[38] W. Qin, J. Qi, Y. Chen, H. Li, X. Wu, Visible light drived N, S -codoped TiO2 photocatalysts grown by microplasma oxidation method, International Journal of Electrochemical Science, 8 (2013) 7680-7686.

[39] A. Bozzi, I. Guasaquillo, J. Kiwi, Accelerated removal of cyanides from industrial effluents by supported TiO2 photo-catalysts, Applied Catalysis B: Environmental, 51 (2004) 203-211.

[40] M.C. Yeber, C. Soto, R. Riveros, J. Navarrete, G. Vidal, Optimization by factorial design of copper (II) and toxicity removal using a photocatalytic process with TiO2 asemiconductor, Chemical Engineering Journal, 152 (2009) 14-19.